JACS
JOURNAL OF THE AMERICAN CHEMICAL SOCIETY
Article
pubs.acs.org/JACS

Selective Photoactivation: From a Single Unit Monomer Insertion Reaction to Controlled Polymer Architectures

Jiangtao Xu,*[,†,‡] Sivaprakash Shanmugam,[†] Changkui Fu,[†] Kondo-Francois Aguey-Zinsou,[§] and Cyrille Boyer*[,†,‡]

[†]Centre for Advanced Macromolecular Design (CAMD), [‡]Australian Centre for NanoMedicine, [§]Materials Energy Research Laboratory (MERLin), School of Chemical Engineering, The University of New South Wales Australia, Sydney, NSW 2052, Australia

Supporting Information

ABSTRACT: Here, we exploit the selectivity of photoactivation of thiocarbonylthio compounds to implement two distinct organic and polymer synthetic methodologies: (1) a single unit monomer insertion (SUMI) reaction and (2) selective, controlled radical polymerization via a visible-light-mediated photoinduced electron/energy transfer-reversible addition−fragmentation chain transfer (PET-RAFT) process. In the first method, precise single unit monomer insertion into a dithiobenzoate with a high reaction yield (>97%) is reported using an organic photoredox catalyst, pheophorbide *a* (PheoA), under red light irradiation (λ_{max} = 635 nm, 0.4 mW/cm^2). The exceptional selectivity of PheoA toward dithiobenzoate was utilized in combination with another catalyst, zinc tetraphenylporphine (ZnTPP), for the preparation of a complex macromolecular architecture. PheoA was first employed to selectively activate a dithiobenzoate, 4-cyanopentanoic acid dithiobenzoate, for the polymerization of a methacrylate backbone under red light irradiation. Subsequently, metalloporphyrin ZnTPP was utilized to selectively activate pendant trithiocarbonate moieties for the polymerization of acrylates under green light (λ_{max} = 530 nm, 0.6 mW/cm^2) to yield well-defined graft co-polymers.

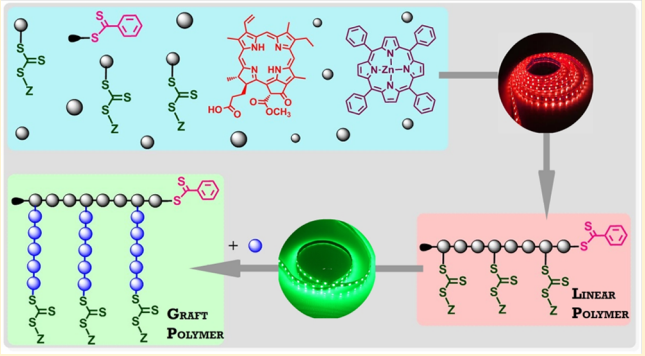

INTRODUCTION

The ability of plants to convert solar energy into chemical energy via photoredox processes (natural photosynthesis) has inspired generations of chemists to try to reproduce such systems.[1−3] Recently, the use of visible-light photoredox catalysis in organic chemistry has enabled the synthesis of known chemical compounds through novel synthetic routes, limiting the formation of side products and eliminating complex purification procedures.[4] More importantly, these photoredox catalysts have also led to the discovery of new chemical transformations. For example, MacMillan and co-workers demonstrated the first direct asymmetric alkylation and β-arylation of ketones and aldehydes.[5−7] Since then, a wide range of chemical reactions have been developed by Stephenson,[8,9] Yoon,[10,11] König,[12,13] and others.[14,15] In addition to the high efficiency of these reactions, which require catalyst concentrations in parts per million amounts, a number of photoredox catalysts have demonstrated additional remarkable properties, including compatibility and selectivity.[16] Taking advantage of its compatibility with a number of common catalytic processes, recent development in the field of visible-light photocatalysis has been dedicated to merging various catalysts to perform complex organic transformation in a single pot.[5,17] For instance, MacMillan and co-workers combined photoredox catalysts with nickel catalysis to couple α-carboxyl sp^3 carbons with aryl halides.[18] In addition to this compatibility, photoredox catalysts are also able to selectively activate specific substrates.[19] Such properties may play an essential role in organic syntheses for the production of added-value chemicals, such as pharmaceuticals, agrochemicals, natural products, pigments, and optoelectronic materials.[16,20]

More recently, the successful implementation of photoredox catalysis in polymer chemistry has led to the development of novel light-mediated polymerizations, which have been used in conventional[21−25] and controlled[26−37] free radical, cationic,[38−42] and ring-opening metathesis[43,44] polymerizations. In contrast to conventional methods, light-mediated polymerizations provide opportunities for spatial and temporal control, which is critical for patterned material fabrication and chemical modification.[15,21,22,26−35,38,43,45−65] Hawker and co-workers pioneered controlled/"living" radical photopolymerization by combining atom transfer radical polymerization (ATRP) with photoredox catalysis.[30,45,66] Inspired by their seminal works, we have developed a living radical polymerization technique involving the reversible deactivation of thiocarbonylthio compounds by photoredox catalysts via a photoinduced electron (Scheme 1) or energy transfer process.[29] A variety of

Received: November 27, 2015
Published: February 25, 2016

DOI: 10.1021/jacs.5b12408
J. Am. Chem. Soc. 2016, 138, 3094−3106

Scheme 1. Proposed Mechanism of PET-RAFT Polymerization (Top) and Photoredox Catalysts (PCs) and RAFT Agents Employed (Bottom) in This Study

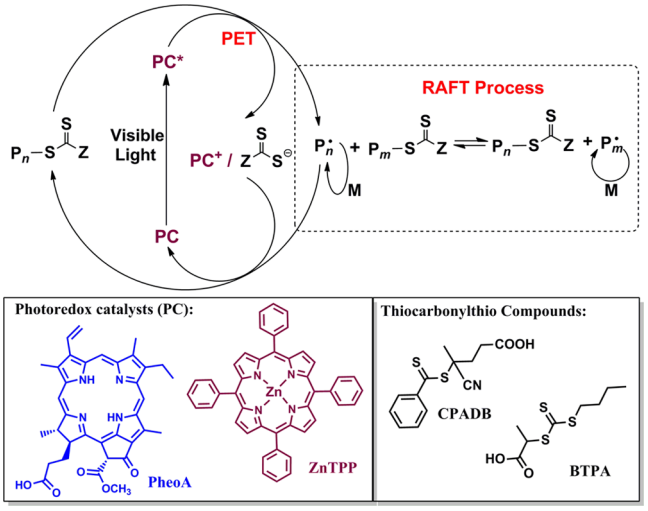

photoredox catalysts, including transition metal complexes,[46,67] organic dyes,[47] metalloporphyrins,[49] and naturally derived catalysts (chlorophyll),[48] have been successfully employed to mediate photoinduced electron/energy transfer-reversible addition−fragmentation chain transfer (PET-RAFT) polymerization. The versatility and effectiveness of this polymerization technique was demonstrated in different media using a broad range of low energy wavelengths in the visible region from blue to near-infrared light (typically, <1 mW/cm^2).[29,68,69] The use of photoredox catalysts in polymer synthesis creates new opportunities to prepare functional polymers. For instance, we were able to achieve dual stereo and temporal control by combining photoredox catalysts with Lewis acids.[70] In another example, we recently reported the first exploitation of selective activation of trithiocarbonates in the presence of zinc tetraphenylporphine (ZnTPP), leading to the fast and controlled polymerization of acrylates, even under open air conditions.[49]

In this article, we exploit selective photoactivation for advanced organic and polymer synthesis. Key photoredox catalyst pheophorbide *a* (PheoA; Scheme 1), an organic porphyrin originating from chlorophyll breakdown, is employed to mediate the PET-RAFT process. In contrast to other conventional photoredox catalysts, it possesses remarkable catalytic activity and selectivity toward specific dithiobenzoates and complements our recent discovery that ZnTPP selectively activates trithiocarbonates.

To illustrate the selectivity of PheoA, we first employ PheoA for the synthesis of organic molecules using a single unit monomer insertion (SUMI) reaction (Scheme 2A).[71−77] With the SUMI reaction proceeding in the presence of monomers such as acrylates, acrylamides, or styrene, the R group of the dithiobenzoate (such as 4-cyanopentanoic acid dithiobenzoate, CPADB; Scheme 1) transitions from a tertiary carbon to a secondary carbon, resulting in a significant change in the stability of the C−S bond. Owing to this chemical structure change, pure monoadducts can be prepared without (or with minimal) purification in a single step. In comparison with a conventional RAFT polymerization system,[78−82] no exogenous initiators are required and the reaction can be performed at room temperature, which eliminates the formation of byproducts from the decomposition of initiator and other side reactions. In addition, the low catalyst concentration (ppm range) negates the need for complex column purification procedures.

Second, we demonstrate the selective activation of dithiobenzoates (CPADB) only by PheoA, in addition to its inability to activate RAFT agents, including trithiocarbonates and xanthates. By combining PheoA with ZnTPP, which presents selectivity toward trithiocarbonates only (Scheme 2B), we prepare complex polymeric architectures via the PET-RAFT process. To illustrate this reaction, a graft co-polymer is prepared via a one-pot, two-step process (Scheme 3). A reaction

Scheme 2. Selective Photoactivation of Thiocarbonylthio Compounds for SUMI Reactions (A) and Controlled Radical Polymerization (B) via the PET-RAFT Process

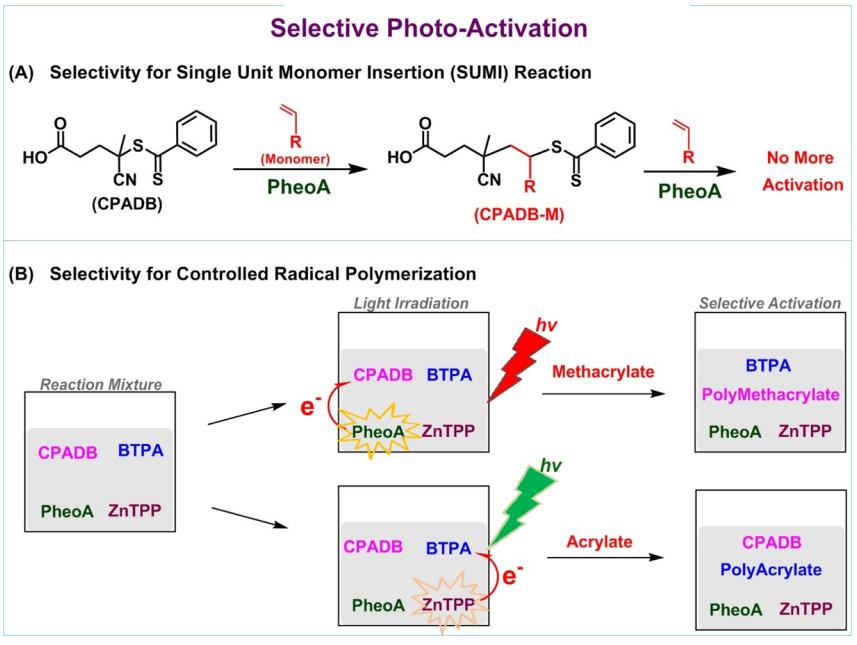

DOI: 10.1021/jacs.5b12408
J. Am. Chem. Soc. 2016, 138, 3094−3106

Scheme 3. Selective Photoactivation for the Preparation of a Graft Co-polymer via a One-Pot, Two-Step Process without Intermittent Postmodification and Purification

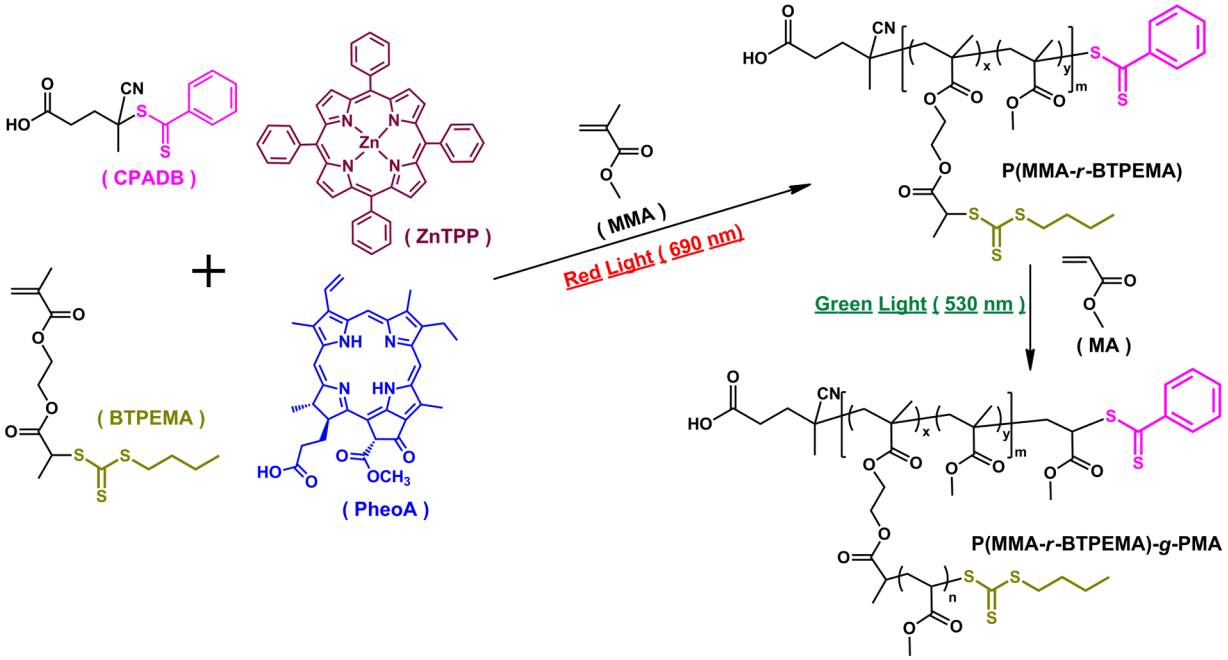

Table 1. Screening Reaction Conditions for Pheophorbide *a* (PheoA)-Regulated PET-RAFT Polymerization of Methyl Methacrylate (MMA) in the Presence of 4-Cyanopentanoic Acid Dithiobenzoate (CPADB) under Red Light Irradiation[a]

no.	[M]/[CPADB]/[PheoA]	[PheoA]/[M] (ppm)	time (h)	α (%)[b]	$M_{n,th}$[c] (g/mol)	$M_{n,GPC}$[d] (g/mol)	M_w/M_n[d]
1	200:1:0.0002	1	12	70	14 280	13 820	1.13
2	200:1:0.0004	2	10	80	16 280	16 310	1.15
3	200:1:0.001	5	10	79	16 180	16 900	1.24
4	200:1:0.002	10	10	80	16 280	17 020	1.32
5[e]	200:1:0.0002	1	36	85	17 260	17 000	1.09
6[f]	200:1:0.0002	1	36	45	9100	8500	1.14
7[g]	200:1:0.02	100	20	70	14 280	13 720	1.18
8[h]	200:1:0.0008	4	24	71	14 440	13 800	1.15

[a]Experimental conditions: solvent, dimethyl sulfoxide (DMSO); light source, red LED light (λ_{max} = 635 nm, 0.4 mW/cm^2). [b]Monomer conversion was determined by ^{1}H NMR spectroscopy. [c]Theoretical molecular weight was calculated using the following equation: $M_{n,th} = [M]_0/[CPADB]_0 \times MW^M \times \alpha + MW^{CPADB}$, where $[M]_0$, $[CPADB]_0$, MW^M, α, and MW^{CPADB} correspond to initial monomer concentration, initial CPADB concentration, molar mass of monomer, conversion determined by ^{1}H NMR, and molar mass of CPADB, respectively. [d]Molecular weight and polydispersity index (M_w/M_n) were determined by GPC analysis calibrated to poly(methyl methacrylate) standards. [e]*fac*-[Ir(ppy)$_3$] photocatalyst; blue LED light (λ_{max} = 460 nm, 0.7 mW/cm^2). [f]Ru(bpy)$_3$Cl$_2$ photocatalyst; blue LED light. [g]Eosin Y photocatalyst; blue LED light. [h]Chlorophyll *a* photocatalyst; red LED light.

mixture containing two RAFT agents (CPADB and 2-(*n*-butyltrithiocarbonate) propionic acid, BTPA), two orthogonal photoredox catalysts (PheoA and ZnTPP), and monomer (methacrylate) is introduced into a single pot. The first step takes place under red light irradiation (UV−vis absorption of PheoA shown in Figure S1), wherein CPADB is selectively activated by PheoA to afford the formation of the methacrylate backbone, whereas ZnTPP and trithiocarbonate remain dormant and unreactive. Following full consumption of the initial methacrylate monomer, an acrylate is introduced into the pot in tandem with a switch to green light, resulting in the selective activation of BTPA by ZnTPP for the preparation of the side chains (Schemes 2B and 3). By implementing this novel orthogonal approach, only a single pairing of a catalyst and a thiocarbonylthio compound was activated at a time.

RESULTS AND DISCUSSION

Investigation of the Catalytic Activity of PheoA. Preliminary results (Table 1) revealed the catalytic efficiency of PheoA in the activation of a dithiobenzoate, CPADB, for the photopolymerization of methacrylates. The catalytic efficiency was illustrated by the high monomer conversion efficiency (~70% monomer conversion; no. 1, Table 1) after 12 h of light exposure (red light, λ_{max} = 635 nm, 0.4 mW/cm^2) at a very low catalyst concentration (1 ppm catalyst relative to monomer concentration) in the presence of CPADB. Such activity is remarkable in comparison with that of previously used photoredox catalysts, which include transition metal catalysts, such as iridium- and ruthenium-based complexes (nos. 5 and 6, Table 1),[29,67] organic dye eosin Y (no. 7, Table 1),[47] and naturally derived catalyst chlorophyll *a* (no. 8, Table 1).[48] These catalysts required longer polymerization times, typically 24 h, and/or higher catalyst concentrations (>10 ppm) to

DOI: 10.1021/jacs.5b12408
J. Am. Chem. Soc. 2016, 138, 3094−3106

achieve similar monomer conversion. More importantly, the polymerization mediated by PheoA was fairly controlled, as demonstrated by the low polydispersity (1.13) and close agreement between the theoretical and experimental molecular weights (nos. 1 and 2, Table 1).

In the case of higher catalyst concentrations (5 and 10 ppm), polymerization rates did not accelerate as expected (79 and 80% for 5 and 10 ppm, respectively, in 10 h; nos. 3 and 4, Table 1), possibly due to self-quenching at higher concentrations.[83,84] Furthermore, higher polydispersities (1.24 for 5 ppm and 1.32 for 10 ppm) were noted. Therefore, all further polymerizations were performed at catalyst concentrations of less than 2 ppm. Several control polymerizations were conducted without the addition of PheoA or RAFT agent or in the absence of light, and in all of these cases, no polymerizations were noted (Table S1), demonstrating the essential roles of the catalyst, RAFT agent, and light. Methacrylate monomers containing functional groups (*t*-butyl, alcohol, tertiary amine, benzyl, and glycidyl) also proved to be compatible with PheoA, as demonstrated by the good correlation between theoretical and experimental molecular weights and low polydispersities (Table S2).

To demonstrate living polymerization and temporal control, the polymerization kinetics of MMA were investigated via online Fourier transform near-infrared (FTNIR) spectroscopy for 1 ppm PheoA under red light irradiation. The monomer conversion was monitored by following the decrease of the vinylic stretching signal of MMA at 6250−6100 cm^{-1}, as reported previously.[47,67] $Ln([M]_0/[M]_t)$ derived from the monomer conversion was plotted against exposure time. Switching the light OFF or ON resulted in reversible deactivation or reactivation of the polymerization (Figure 1A), indicating temporal

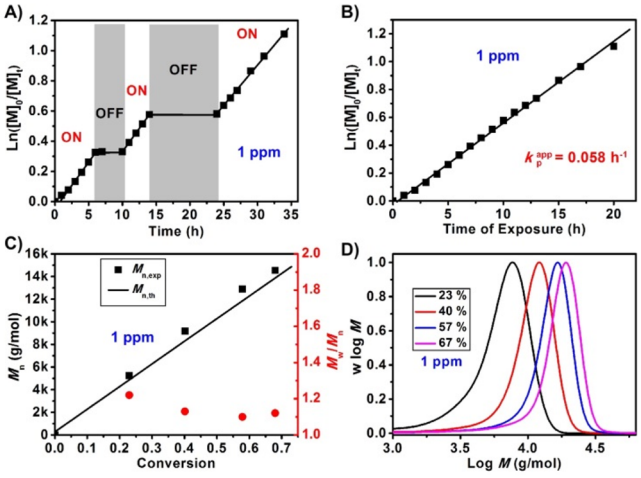

Figure 1. PET-RAFT polymerization of MMA using CPADB and PheoA as the photoredox catalyst in the presence (ON) or in the absence (OFF) of light: (A) ON/OFF experiment; (B) $ln([M]_0/[M]_t)$ vs time of exposure; (C) $M_{n,exp}$ (■), $M_{n,th}$ (−), and M_w/M_n (●) vs conversion; (D) molecular weight distributions at different monomer conversions. Reaction conditions: toom temperature; red LED light (λ_{max} = 635 nm, 0.4 mW/cm^2); [MMA]/[CPADB]/[PheoA] = 200:1:0.0002 (1 ppm PheoA relative to monomer concentration); $[MMA]_0$ = 4.7 mol/L; PMMA standard for molecular weight calibration.

control. In the absence of light (OFF), the polymerization immediately stops, which was attributed to rapid deactivation by the catalyst. In addition, the linear plot of $ln([M]_0/[M]_t)$ versus exposure time (Figure 1B) revealed a constant radical concentration, which confirmed that the catalytic activity of PheoA was highly stable under these conditions. The good accord between the experimental and theoretical number-average molecular weights ($M_{n,exp}$ and $M_{n,th}$) as well as the linear increase in M_n versus monomer conversion, low polydispersity (Figure 1C), and symmetrical gel permeation chromatography (GPC) curves (Figure 1D) further verified the living features of the process.

PheoA for Selective Polymerization via Activation of 4-Cyanopentanoic Acid Dithiobenzoate (CPADB). During this investigation, we discovered that PheoA exhibited a remarkable selectivity toward CPADB. Other investigated RAFT agents listed in Scheme S1 include dithiobenzoates (2-cyano-2-propyl benzodithioate, CPD, and cumyl dithiobenzoate, CDB), trithiocarbonates (2-(*n*-butyltrithiocarbonate)-propionic acid, BTPA, 2-(dodecylthiocarbonothioylthio)-2-methylpropionic acid, DDMAT, and 3-benzylsulfanylthiocarbonylthiosulfanyl propionic acid, BSTP), and xanthate (methyl 2-[(ethoxycarbonothioyl)sulfanyl]propanoate). When we tested these RAFT agents with their compatible monomer families, such as acrylates, acrylamides, and vinyl acetate, negligible monomer conversion was surprisingly detected (nos. 1−9, Table 2). This exceptional catalytic selectivity was attributed to a plausible specific interaction between CPADB and PheoA, which is discussed and investigated in the following section.

To prove the specific selectivity of PheoA, we carried out polymerizations in the presence of two different families of RAFT agent: a dithiobenzoate, CPADB, and a trithiocarbonate, BTPA or 2-(dodecylthiocarbonothioylthio)-2-methylpropionic acid (DDMAT) (Scheme S1). The experiments were performed under red light irradiation (λ_{max} = 635 nm, 0.4 mW/cm^2) using the formulation of [MMA]/[CPADB]/[BTPA]/[PheoA] = 200:0.5:0.5:0.0004 (no. 10, Table 2). The results showed controlled polymerization with low polydispersity (1.14) and relatively high MMA conversion (~50%) after 20 h. In the case of DDMAT (no. 11, Table 2), a faster polymerization (50% at 12 h reaction) was observed. Remarkably, in both polymerizations, the experimental molecular weights corresponded to the theoretical values calculated using CPADB as the only chain transfer agent, suggesting the absence of trithiocarbonate activation or chain transfer to trithiocarbonate. To confirm these unexpected results, a kinetic study was carried out to follow the evolution of experimental molecular weight and polydispersity versus monomer conversion (Figure S2). The kinetics for the CPADB/BTPA system, surprisingly, revealed the selective activation of CPADB for the polymerization of MMA through the comparable evolution of molecular weights between experimental and theoretical values calculated using CPADB only. This result suggests that BTPA did not participate in the polymerization. To confirm this result, we decided to purify the polymer by several precipitations and carried out further analysis. The purified polymer displayed a pink color characteristic of dithiobenzoates, whereas the supernatant from precipitation presented a light yellow color characteristic of trithiocarbonates. This qualitative observation tends to show that the trithiocarbonates were not reacted. This result was also verified by UV−vis and NMR spectroscopies. The UV−vis spectrum of the purified product (black line, Figure 2) showed only the presence of dithiobenzoate group and the absence of signal at 423 nm characteristic of trithiocarbonate group. Furthermore, ^1H NMR analysis (Figure S3)

DOI: 10.1021/jacs.5b12408
J. Am. Chem. Soc. 2016, 138, 3094−3106

Table 2. PheoA-Regulated PET-RAFT Polymerization of Different Monomer Families and Various RAFT Agents under Red Light Irradiation[a]

no.	[M]/[RAFT]/[PheoA]	monomer	RAFT agent	[PheoA]/[M] (ppm)	time (h)	α (%)[b]	$M_{n,th}$[c] (g/mol)	$M_{n,GPC}$[d] (g/mol)	M_w/M_n[d]
1	200:1:0.002	MMA	DDMAT	10	10	5			
2	200:1:0.0002	MMA	CDB	1	24	<1			
3	200:1:0.0002	MMA	CDB	10	24	1			
4	200:1:0.0002	MMA	CPD	1	24	10			
5	200:1:0.0002	MMA	CPD	10	24	4			
6	200:1:0.002	MA	BTPA	10	8	0			
7	200:1:0.002	MA	BSTP	10	8	0			
8	200:1:0.002	DMA	BTPA	10	6	5			
9	200:1:0.002	VAc	xanthate	10	24	0			
10[e]	200:(0.5/0.5):0.0004	MMA	CPADB/BTPA (0.5/0.5)	2	20	51	20 680[f]	21 630	1.14
11[e]	200:(0.5/0.5):0.0002	MMA	CPADB/DDMAT (0.5/0.5)	1	12	50	20 280[f]	19 790	1.13

[a]Experimental conditions: solvent, dimethyl sulfoxide (DMSO); light source, red LED light (λ_{max} = 635 nm, 0.4 mW/cm^2). Abbreviations: VAc, vinyl acetate; DMA, *N*,*N*′-dimethylacrylamide; CPD: 2-cyano-2-propyl benzodithioate; CDB, cumyl dithiobenzoate; xanthate, methyl 2-[(ethoxycarbonothioyl)sulfanyl]propanoate; BTPA, 2-(*n*-butyltrithiocarbonate)-propionic acid; DDMAT, 2-(dodecylthiocarbonothioylthio)-2-methylpropionic acid; BSTP, 3-benzylsulfanylthiocarbonylthiosulfanyl propionic acid. [b]Monomer conversion was determined by ^{1}H NMR spectroscopy. [c]Theoretical molecular weight was calculated using the following equation: $M_{n,th} = [M]_0/[RAFT]_0 \times MW^M \times \alpha + MW^{RAFT}$, where $[M]_0$, $[RAFT]_0$, MW^M, α, and MW^{RAFT} correspond to initial monomer concentration, initial RAFT agent concentration, molar mass of monomer, conversion determined by ^{1}H NMR, and molar mass of RAFT agent, respectively. [d]Molecular weight and polydispersity index (M_w/M_n) were determined by GPC analysis calibrated to poly(methyl methacrylate) or polystyrene standards. [e]The RAFT agent is the mixture of CPADB and BTPA (or DDMAT) (0.5:0.5, mol/mol). [f]Theoretical molecular weight was calculated on initiation of CPADB only.

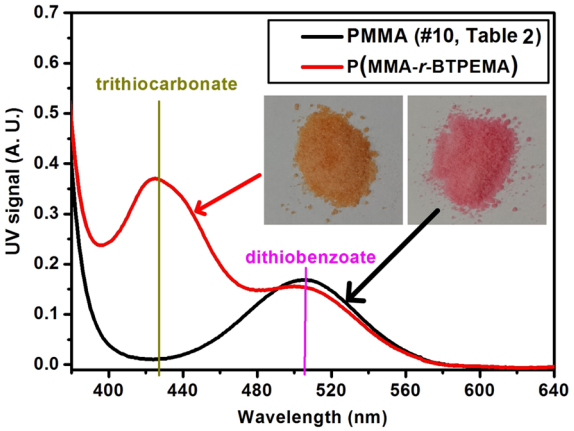

Figure 2. UV−vis spectra for PMMA prepared by selective activation of CPADB for MMA polymerzation mediated by PheoA (black line; no. 10, Table 2) and purified macroinitiator P(MMA-*r*-BTPEMA) (red line) to show the absorption of dithiobenzoate and trithiobenzoate in the visible region. The inset pictures show the color of the purified polymers: PMMA (no. 10, Table 2) (right) and purified macroinitiator P(MMA-*r*-BTPEMA) (left) prepared in the Selective Photoactivation To Build a Graft Co-polymer through a One-Pot, Two-Step Process section.

of the purified product confirmed the presence of only the dithiobenzoate moiety. Indeed, the absence of BTPA in the polymer structure was demonstrated by the absence of a signal at 3.2 ppm characteristic of CH_2 in the adjacent position to the trithiocarbonate group, which again supports that BTPA was not activated or reacted. Calculations of the molecular weight using NMR were performed by comparing the characteristic signals of CPADB at 7.2, 7.4, and 7.8 ppm and methyl methacrylate (OCH_3) at 3.5 ppm. The good agreement of the molecular weight between NMR and GPC ($M_{n,NMR}$ = 23 110 g/mol vs $M_{n,GPC}$ = 21 630 g/mol) supports the notion that only CPADB was activated. The supernatant was also concentrated and analyzed by ^{1}H NMR, which clearly showed the characteristic signals of unreacted BTPA (Figure S4). The integrity of the dithiobenzoate group was further demonstrated by successful chain extension with MMA using purified polymer as the macroinitiator (Figure S5).

As a comparison, we performed a conventional RAFT polymerization using AIBN as a thermal initiator in the presence of the same RAFT agents. As expected, thermally initiated RAFT polymerization using CPADB in the presence of DDMAT (or BTPA) showed no signs of selectivity (Table S3). Although low polydispersities were obtained, the experimental molecular weights were much lower compared with the theoretical values based on CPADB only, suggesting the presence of activation of and chain transfer to trithiocarbonate. After purification by several precipitations, the ^{1}H NMR signal of the proton (-S-CH_2-) adjacent to the thiocarbonylthio of DDMAT was also observed at 3.21 ppm (Figure 3), whereas it was not detectable for the polymerization mediated using the PET-RAFT process. This unique selectivity observed in the PET-RAFT process can be attributed to its distinctive mechanism in comparison with that of the conventional RAFT process. Indeed, we previously established that PET-RAFT polymerization was a combination of the PET and RAFT processes (Scheme 1).[29] The PET process governs the carbon radical activation and deactivation, whereas the RAFT process facilitates radical exchanges between the dormant and active polymer chains. These two processes cooperatively afford living radical behavior with excellent control. However, in the current study, we hypothesize that the PET process dominates the entire polymerization and the RAFT process (mainly chain transfer) is effectively suppressed because of an interaction between PheoA and CPADB.

Mechanistic Insights into the Selectivity of PheoA. The unique photophysical properties of PheoA in comparison with those of other photoredox catalysts may explain its higher efficiency. It possesses a very high intersystem crossing rate and triplet quantum yield compared with its fluorescence rate and

DOI: 10.1021/jacs.5b12408
J. Am. Chem. Soc. 2016, 138, 3094−3106

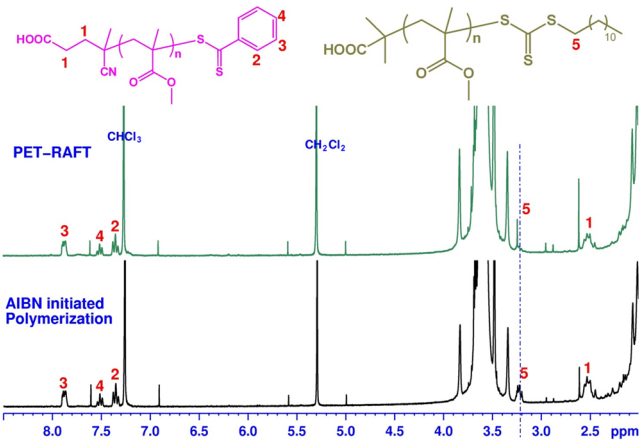

Figure 3. ^{1}H NMR spectra (300 MHz, $CDCl_3$) of purified PMMA prepared by PheoA-mediated PET-RAFT polymerization (green curve, top) and AIBN-initiated RAFT polymerization (black curve, bottom) in the presence of a CPADB/DDMAT (1:1, mol/mol) mixture as the RAFT agent. PET-RAFT (no. 11, Table 2): [MMA]/[CPADB]/[DDMAT]/[PheoA] = 200:0.5:0.5:0.0002 (1 ppm PheoA relative to monomer concentration); $[MMA]_0$ = 4.7 mol/L. AIBN-initiated polymerization (no. 1, Table S3): [MMA]/[CPADB]/[DDMAT]/[AIBN] = 200:0.5:0.5:0.1; $[MMA]_0$ = 4.7 mol/L.

Table 3. Photophysical Data for Pheophorbide *a* (PheoA)

photocatalyst	k_F [10^7 s^{-1}][a]	k_{ISC} [10^8 s^{-1}][a]	Φ_{S1}[a]	Φ_{T1}[a]
PheoA	4.4	1.2	0.2	0.8

[a] k_F, k_{ISC}, Φ_{S1}, and Φ_{T1} correspond to fluorescence rate, intersystem crossing rate, singlet quantum yield, and triplet state quantum yield, respectively.[85]

singlet quantum yield (Table 3). These properties favor an electron generated by photoexcitation to remain longer in the triplet state, which consequently increases the probability for an electron transfer event from the π-conjugated excited state of PheoA to RAFT agents.

To investigate the reaction mechanism between PheoA and CPADB, two different quenching experiments were performed to demonstrate that a PET process is occurring between PheoA and CPADB. The first set of experiments involved measuring fluorescence quenching by titrating increasing amounts of RAFT agents in the presence of a fixed concentration of PheoA (Figures S6 and S7), and the second set of experiments involved measuring quenching after irradiation of PheoA and RAFT agents at a molar ratio of 1:150 under red light (Figure 4). Both techniques are commonly employed to demonstrate a PET or energy transfer process between two molecules.[84,86−88] These experiments revealed that fluorescence of PheoA, upon excitation at λ_{max} = 635 nm, was quenched only in the presence of CPADB (Figure 4A). In the presence of BTPA (Figure 4B) or CPD (Figure 4C), we did not observe quenching in any experiments, which confirmed the absence of the electron or energy transfer process between BTPA (or CPD) and PheoA.

To confirm that the transfer of an electron is possible between PheoA and CPADB, we measured the ground state oxidation potential using cyclic voltammetry (CV) of PheoA in DMSO. CV experiments were recorded using glass carbon (BASI) electrodes in anhydrous DMSO containing 0.1 M tetrabutylammonium tetrafluoroborate as the electrolyte. First, we determined that the reduction potential (Pheo/Pheo$^-$) was in good accord with the previous values reported in the literature.[89] Then, we assessed the first electron oxidation potential ($PheoA^+$/PheoA) of PheoA to be +0.3 V (vs Ag/AgCl) (Figure S8) by CV. According to the previously reported equation ($E^\circ_{PheoA^+/PheoA^*} = E^\circ_{PheoA^+/PheoA} - E_{h\nu} = E^\circ_{PheoA^+/PheoA} - \frac{hc}{\lambda_{max}}$),[90] the excited state oxidation potential ($PheoA^+$/PheoA*) of PheoA can be estimated to be around −1.4 V (vs saturated calomel electrode, SCE) based on ground state value. As the oxidation potential of excited PheoA is much lower than the reduction potentials of CPADB (−0.4 V vs SCE),[29,91] the probability for an electron transfer from PheoA to CPADB is deemed thermodynamically favorable.

In the literature, many reports[92−94] have shown that the proximity of an electron donor and acceptor enhances their catalytic activities. First, ^{1}H NMR analysis was utilized to investigate the presence of a possible interaction between CPADB and PheoA. The ^{1}H NMR spectrum for the mixture of PheoA and CPADB (1:2, mol/mol) revealed the presence of weak dynamic association between PheoA and CPADB in DMSO, evidenced by the clear shift in the proton signals of PheoA (Figure 5). Additionally, UV−vis spectra (Figure 6) displayed a marginal blue shift (3 nm) of PheoA in the presence of CPADB absorption at 670 nm before and after 6 h of light irradiation of the polymerization mixture. This interaction could be attributed to the formation of hydrogen bonding between the pyrrole and acid groups of CPADB, which was supported by the shift of the proton signals of pyrrole in the NMR spectra when comparing CPADB to the CPADB/PheoA mixture (Figure 5).

Selective Photoactivation of 4-Cyanopentanoic Acid Dithiobenzoate (CPADB) for Single Unit Monomer

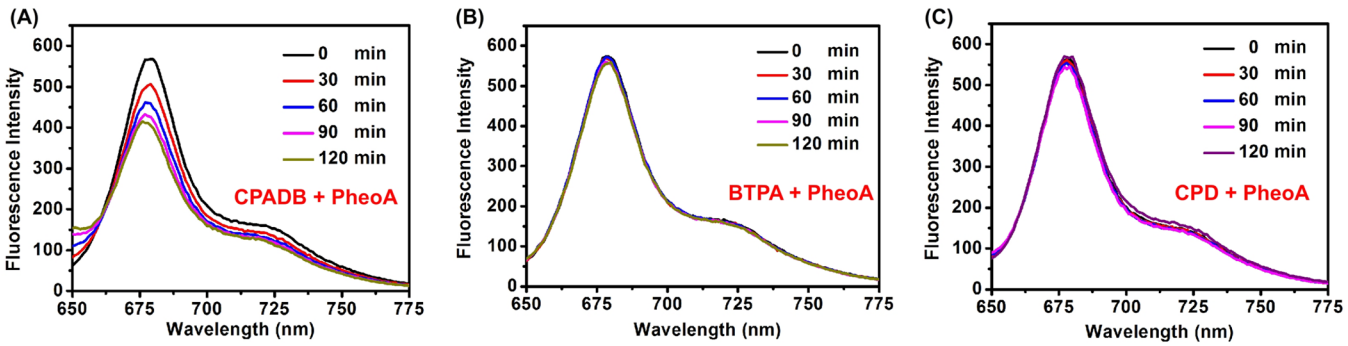

Figure 4. Fluorescence emission spectra of 33.8 μM Pheo A in DMSO in the presence of a fixed concentration of CPADB (A), BTPA (B), and CPD (C) under red light irradiation (λ_{max} = 635 nm, 0.4 mW/cm^2) at different time points with a molar ratio of [PheoA]/[RAFT] = 1:150.

DOI: 10.1021/jacs.5b12408
J. Am. Chem. Soc. 2016, 138, 3094−3106

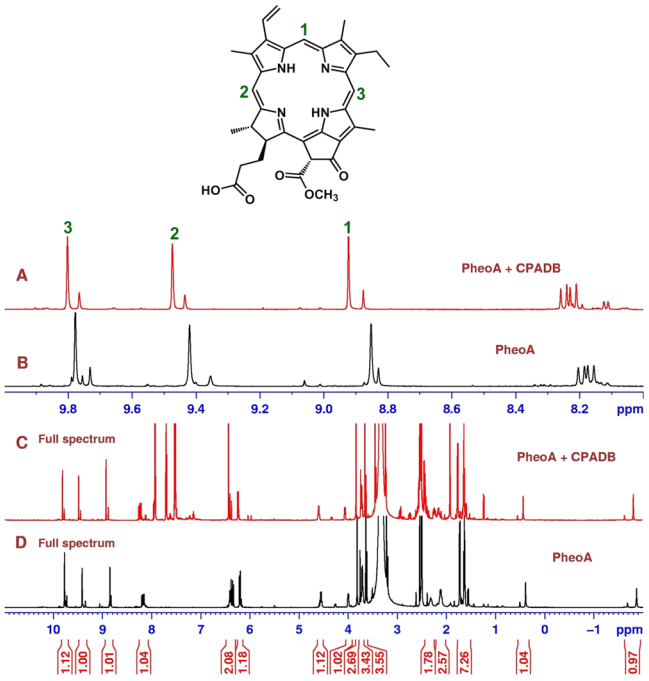

Figure 5. Enlarged (A, B) and full (C, D) ^{1}H NMR spectra (600 MHz, DMSO-d_6) for PheoA (B, D) and the PheoA and CPADB (1:2, mol/mol) mixture (A, C) in the presence of air.

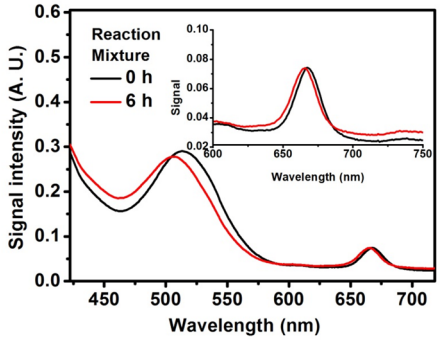

Figure 6. UV−vis absorption of the polymerization mixture in DMSO before (black curve) and after (red curve) red light irradiation. [MMA]/[CPADB]/[PheoA] = 200:1:0.0004 (2 ppm PheoA relative to monomer concentration); $[MMA]_0$ = 4.7 mol/L; light source: 635 nm red LED light, 0.4 mW/cm^2.

Insertion (SUMI) Reactions. The high catalytic efficiency of PheoA for CPADB was exploited to perform SUMI into RAFT agents for the preparation of a monoadduct. SUMI is an effective approach used to control monomer sequence in synthetic polymer materials or for the functionalization of polymer chain ends.[71,77,80,95−97] Monomer sequence regulation plays a key role in biology and is a prerequisite for crucial features of life, such as heredity, self-replication, complex self-assembly, and molecular recognition.[80,93] Developing synthetic polymers containing precise monomer sequences is an important area of research. Previous reports required the use of stoichiometric amounts of monomer and RAFT agent to avoid the formation of oligomers (multiadducts), except for monomers such as maleic anhydride and maleimides that do not undergo homopolymerization.[78] In the case of high molar ratios of monomer to RAFT agent, it is necessary to control parameters such as reaction time and temperature to reduce or avoid the formation of multiadducts. Isolation of the pure monoadduct also requires laborious purifications to remove initiator-derived byproducts and multiadducts. The initial RAFT agent can be effectively activated and deactivated through the PET process in the presence of low concentrations of PheoA. The use of photoredox catalysts avoids the use of initiator species and the consequential formation of initiator-derived byproducts. More importantly, the activation via PheoA is highly dependent on the structure of the R group of the RAFT agent. As illustrated in Scheme 4, following the SUMI reaction with acrylate,

Scheme 4. SUMI into CPADB via Visible-Light-Mediated Selective Photoactivation

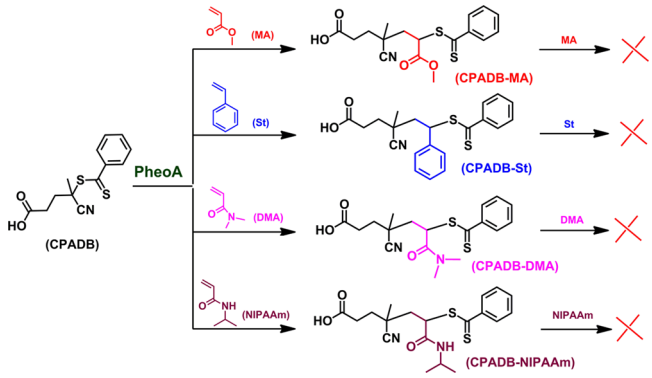

acrylamide, and styrene in the presence of CPADB, the structure of the dithiobenzoate R group is radically changed from a tertiary carbon to a secondary carbon, resulting in a significant change in the stability of the C−S bond. Such changes affect the PET activation process by PheoA. Indeed, CPADB is rapidly activated in the presence of PheoA, but after one monomer addition, the resultant dithiobenzoate cannot be reactivated by PheoA anymore. This appears to be a convenient method to selectively insert one monomer unit into CPADB.

The preliminary results shown in Table 4 demonstrated successful SUMI into CPADB using different monomer families such as styrene, acrylates, and acrylamides (nos. 1−4, Table 4). Excess monomer, typically [monomer]/[RAFT] = 20:1, was employed to obtain faster reaction rates (typically, 20 h). When lower ratios were utilized (i.e., [monomer]/[RAFT] = 1:1), longer reaction times were required. Only a single monomer unit was inserted into CPADB, which was confirmed by ^{1}H NMR (Figure 7 and Figures S9−15) and GPC (Figure 8). ^{1}H NMR spectra (Figure 7) of crude product (after evaporation of monomer and solvent under reduced pressure) for the reaction of CPADB with MA displays a single unit addition, CPADB-MA. The ^{1}H NMR spectrum indicates that the SUMI reaction proceeded with negligible side reactions via a PET-RAFT process mediated by PheoA. The CPADB conversion was calculated by comparing the ratio of the integration of the proton signal at δ 7.92 ppm to that at δ 8.0, which corresponds to the signal of the benzyl group before and after the reaction, respectively. The good correlation between the integrals of the methyl groups in the monomer unit (δ 3.83 ppm) and R group fragment of the RAFT agent (δ 1.4−1.6 ppm) demonstrate the synthesis of a 1:1 mixture of two diastereomers for CPADB-MA. The purified product of CPADB-MA by column chromatography did not show any difference, eliminating the need for purification via column chromatography. SUMI reactions with acrylamides also yielded high-purity mono-

DOI: 10.1021/jacs.5b12408
J. Am. Chem. Soc. 2016, 138, 3094−3106

Table 4. Screening Conditions for SUMI Reactions via Selective Photoactivation[a]

no.	[Monomer]/[RAFT]/[catalyst or AIBN]	RAFT agent	monomer	products	CPADB conversion (%)[b]	isolated yield (%)[c]
1[d]	20:1:0.0004	CPADB	MA	CPADB-MA	98	92
2[d]	5:1:0.0004	CPADB	St	CPADB-St	98	90
3[d]	20:1:0.0004	CPADB	DMA	CPADB-DMA	99	91
4[d]	20:1:0.0008	CPADB	NIPAAm	CPADB-NIPAAm	97	90
5[d]	20:1:0.0004	CPADB	MMA	Oligo-PMMA		
6[e]	20:1:0.0004	CPADB	MA	CPADB-MA	30	
7[f]	20:1:0.2	CPADB	MA	Oligo-PMA		
8[g]	20:1:0	CPADB	MA		10	
9[d]	20:1:0.0004	PMMA[h]	*n*BA	PMMA-*n*BA	97	95

[a]Experimental conditions: solvent dimethyl sulfoxide, (DMSO); 20 h light irradiation or thermal reaction. Abbreviations: St, styrene; DMA, *N*,*N*′-dimethylacylamide; NIPAAm, *N*-isopropylacrylamide; *n*BA, *n*-butyl acrylate. [b]Determined by ^{1}H NMR for crude products. [c]Products were purified by column chromatography. [d]PheoA photoredox catalyst; red LED light source (λ_{max} = 635 nm, 0.4 mW/cm^2). [e]Ir(ppy)$_3$ photoredox catalyst; blue LED light source (λ_{max} = 460 nm, 0.7 mW/cm^2). [f]Thermally initiated polymerization using AIBN as the initiator (70 °C). [g]No photoredox catalyst; blue LED light source (λ_{max} = 460 nm, 12 mW/cm^2); 26 h light irradiation. [h]PMMA macro-RAFT was prepared by PET-RAFT polymerization of MMA mediated by PheoA. $M_{n,GPC}$ = 7100 g/mol.

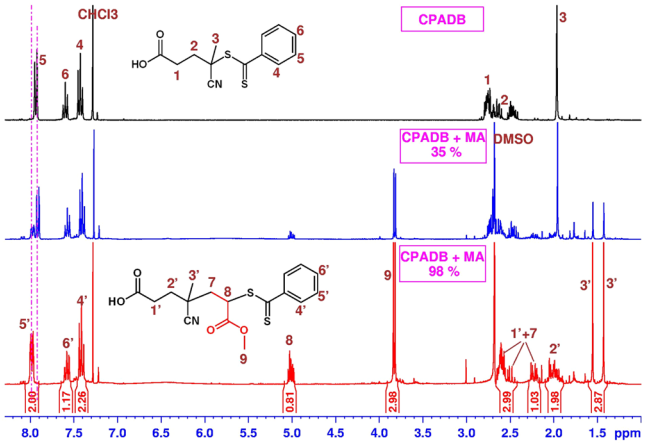

Figure 7. ^{1}H NMR spectra for monitoring the SUMI reaction between dithiobenzoate (CPADB) and monomer (MA) at different CPADB conversions: 0%, black curve on the top; 35%, blue curve in the middle; and 98%, red curve at the bottom.

adducts without the need of column purification. GPC curves (Figure 8) of these crude products revealed the absence of any dimer shoulders, demonstrating excellent SUMI reaction profiles and high CPADB conversion. In the case of *N*-isopropylacrylamide (NIPAAm), a simple purification step by column chromatography was required owing to the high boiling point of the monomer. Despite this, the CPADB-NIPAAm monoadduct was isolated in high yields.

Single unit monomer addition of styrene into CPADB was performed (no. 2, Table 4) using a lower monomer-to-RAFT ratio (5:1) owing to partial double monomer unit insertion at higher ratios (20:1), as evidenced by the shoulder in the GPC trace (Figure S16). As expected, the attempt to prepare SUMI of MMA gave an oligomeric product (no. 5, Table 4), which was attributed to repeated activations without selectivity. In comparison, lower monoaddition conversion (30%; no. 6, Table 4) was obtained when Ir(ppy)$_3$ was employed as the photoredox catalyst in the presence of MA under blue light irradiation, which is attributed to the quenching of Ir(ppy)$_3$ with CPADB at 460 nm. This result illustrates the exceptional catalytic efficiency of PheoA. In another comparison, we performed a SUMI reaction via conventional RAFT polymerization using [monomer]/[RAFT] = 20:1. Expectedly, the thermally initiated polymerization of MA (no. 7, Table 4), using AIBN as initiator and CPADB, gave poor control over single unit insertion, resulting in the formation of oligomers, as shown by GPC (Figure S17) and ^{1}H NMR (Figure S18). To demonstrate the importance of the catalyst (PheoA) in this process, catalyst-free photopolymerization[98,99] using CPADB under high intensity blue light (λ = 460 nm, 12 mW/cm^2) was performed. After 26 h of light exposure, only 10% CPADB conversion (no. 8, Table 4) and an inefficient SUMI reaction (see Figure S19 for the ^{1}H NMR spectrum of the crude product) were observed. In summary, only the PheoA-mediated PET-RAFT approach was able to afford efficient SUMI reactions. In addition, this technique has been successfully

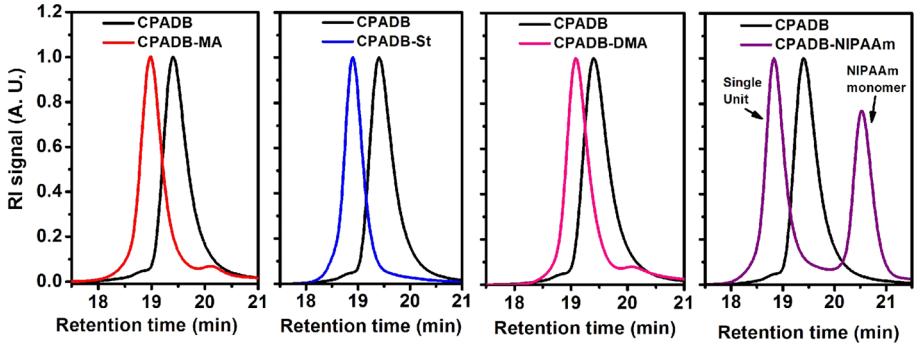

Figure 8. GPC curves of the crude SUMI products of different monomers (MA, St, DMA, and NIPAAm) to RAFT agent, CPADB, prior to purification showing the absence of multiple insertion products (oligomers).

DOI: 10.1021/jacs.5b12408
J. Am. Chem. Soc. 2016, 138, 3094−3106

implemented for the specific addition of a single unit of *n*-butyl acrylate to a macro-RAFT PMMA (no. 9, Table 4).

Selective Photoactivation To Build a Graft Co-polymer through a One-Pot, Two-Step Process. In our previous work,[49] we demonstrated that ZnTPP selectively activated trithiocarbonates in the PET-RAFT process. In light of the discovery of the specificity of PheoA, we sought to employ the orthogonal reactivity of these two catalysts, under different wavelengths, for the preparation of complex polymer architectures. As an example, a graft co-polymer was prepared in a one-pot reaction through selective photoactivation using two different wavelengths. Using conventional living radical polymerization, the synthesis of graft co-polymers requires several steps (including postmodifications and purifications) and/or the combination of different polymerization techniques,[58,100−104] such as RAFT and ATRP.[105,106] In this work, we proposed the synthesis of model graft co-polymers (PMMA-*g*-PMA) using only one technique through the selective activation of two different RAFT agents in one pot without intermediate purification. Two different monomers were sequentially polymerized to fabricate the polymer backbone and graft chain, respectively, by switching the wavelength of the light (Scheme 3). Under red light irradiation, PheoA specifically activated the dithiobenzoate, resulting in the polymerization of the methacrylate backbone. Following the addition of acrylate monomer, the light was switched to green to activate the trithiocarbonate using ZnTPP as the photoredox catalyst, resulting in the formation of polyacrylate graft chains.

To demonstrate this orthogonal selectivity and rule out any potential side reactions (cross activation or overlapped light absorption) by these two catalysts, several control experiments were carried out. First, two different wavelengths were selected for each catalyst. At 690 nm, ZnTPP does not absorb, whereas PheoA presents strong absorption in this region (Figure 9). We

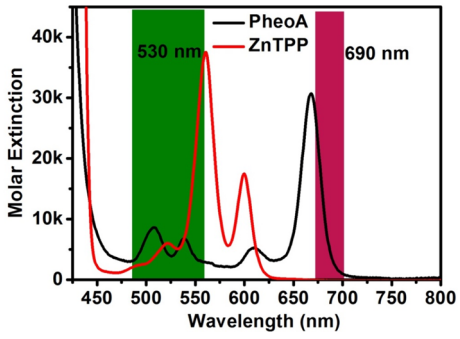

Figure 9. UV−vis absorption and molar extinction of PheoA and ZnTPP for screening the activation light wavelength for selective polymerization activation.

decided to test ZnTPP under 690 nm red light irradiation (2 mW/cm^2) using the following formulations: [MMA]/[BTPA]/[ZnTPP] = 200:1:0.01 and [MMA]/[CPADB]/[ZnTPP] = 200:1:0.01. In both cases, low monomer conversions (8 and 0%, respectively, after 24 h) were determined by NMR, which suggests negligible activation of the RAFT agent via ZnTPP at this wavelength. On the other hand, at 530 nm, PheoA displays low absorption (Figure 9), whereas ZnTPP presents maximum absorption in this region. The activation ability of PheoA at 530 nm was therefore tested using PheoA with either MA and MMA, formulated as [MMA]/[CPADB]/[PheoA] = 200:1:0.0004 and [MA]/[CPADB]/[PheoA] = 200:1:0.0004, respectively. Both reactions revealed low monomer conversions (3 and 0%, respectively) after 24 h of irradiation under green light (0.6 mW/cm^2), which can be ascribed to the light being quenched by CPADB in the green region (Figure 6). Therefore, 690 nm red light was employed to excite PheoA to selectively activate CPADB, whereas 530 nm green light was used for ZnTPP and BTPA.

Next, the compatibility of these two photoredox catalysts needed to be confirmed to prevent photodeactivation through energy or electron transfer from one catalyst to the other. Therefore, two model reactions were carried out: (1) selective activation of CPADB by PheoA to polymerize MMA under 690 nm red light irradiation in the presence of BTPA and ZnTPP and (2) selective activation of BTPA by ZnTPP to polymerize MA under 530 nm green light irradiation in the presence of CPADB and PheoA. As demonstrated in the Investigation of the Catalytic Activity of PheoA section, PheoA is an efficient catalyst for mediating the PET-RAFT polymerization of MMA at 635 nm. The shift of red light to a higher wavelength (690 nm) slightly affects the polymerization rate due to the lower absorption of PheoA in this region. Indeed, polymerization with the formulation [MMA]/[BTPA]/[CPADB]/[PheoA]/[ZnTPP] = 200:5:1:0.0004:0.02 (2 ppm PheoA and 100 ppm ZnTPP relative to monomer concentration) proceeded smoothly to reach 79% conversion after 23 h at 690 nm red light irradiation. The precipitated polymer from the reaction mixture appears pink in color and did not show any trithiocarbonate moieties from BTPA in the ^{1}H NMR spectrum (Figure S20), as expected with our previous findings. The concentrated supernatant of this reaction mixture also contained unreacted BTPA, as determined by ^{1}H NMR (Figure S21).

The model polymerization of MA under green light (λ_{max} = 530 nm, 0.6 mW/cm^2) in the presence of CPADB/BTPA (0.25:1, mol/mol), ZnTPP, and PheoA in DMSO was investigated using the formulation [MA]/[CPADB]/[BTPA]/[PheoA]/[ZnTPP] = 400:0.25:1:0.0008:0.02 (2 ppm PheoA and 50 ppm ZnTPP relative to monomer concentration). Higher ratios of [CPADB]/[BTPA] were tested, which nevertheless resulted in a very long induction period (>24 h). The kinetic study showed that polymerization proceeded quickly after a 380 min induction period (Figure S22A). The polymerization displayed characteristics of living polymerization with a linear increase in the molecular weight with monomer conversion, accompanied by a low polydispersity (<1.10). The theoretical molecular weight, calculated using BTPA as the only chain transfer agent, was in good agreement with the experimental values measured by GPC (Figure S22B) and NMR (Figure S23). The possible radical chain transfer to CPADB was suppressed owing to selective reactivation. ^{1}H NMR analysis of the purified polymer (Figure S23) revealed no dithiobenzoate moieties, which further confirmed that no introduction of CPADB into the polymer chains had occurred. The concentrated supernatant after precipitation clearly showed the presence of dithiobenzoate (Figure S24). Successful chain extension of the purified product with MA indicated high end group fidelity (Figure S25). The unimodal molecular weight distribution (Figure S22C) demonstrated that the presence of CPADB and PheoA did not affect the living character of the polymerization, except for a prolonged induction period.

Having demonstrated by two model reactions that PheoA and ZnTPP selectively activate/deactivate only CPADB and BTPA, respectively, we decided to take advantage of this ability

DOI: 10.1021/jacs.5b12408
J. Am. Chem. Soc. 2016, 138, 3094−3106

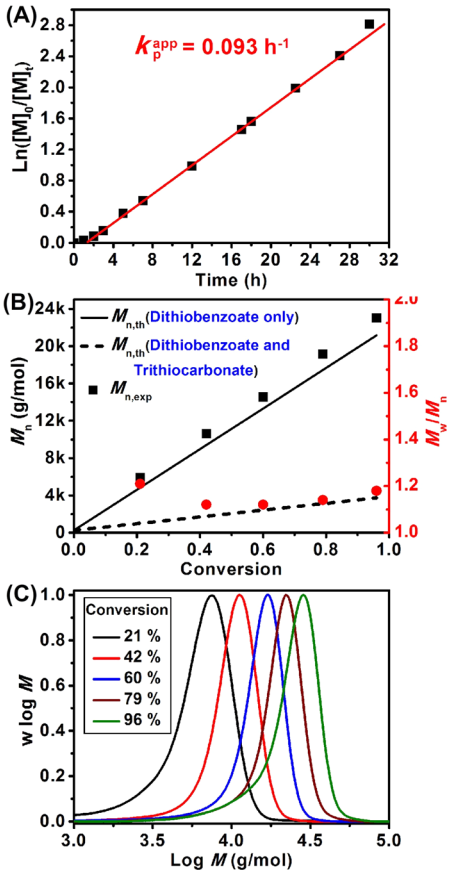

Figure 10. Kinetic study of the co-polymerization of MMA and BTPEMA using CPADB as the chain transfer agent in the presence of PheoA and ZnTPP under 690 nm red light irradiation (λ_{max} = 690 nm, 2 mW/cm^2): (A) ln([M]$_0$/[M]$_t$) vs time; (B) $M_{n,exp}$ (■), $M_{n,th}$ based on dithiobenzoate (CPADB) only (solid line), $M_{n,th}$ based on dithiobenzoate and trithiocarbonate moieties (dashed line), and M_w/M_n (●) vs conversion; (C) molecular weight distributions at different monomer conversions. Reaction conditions: [MMA]/[BTPEMA]/[CPADB]/[PheoA]/[ZnTPP] = 200:5:1:0.0004:0.02 (2 ppm PheoA and 100 ppm ZnTPP relative to monomer concentration); [MMA]$_0$ = 4.7 mol/L; PMMA standard for molecular weight calibration.

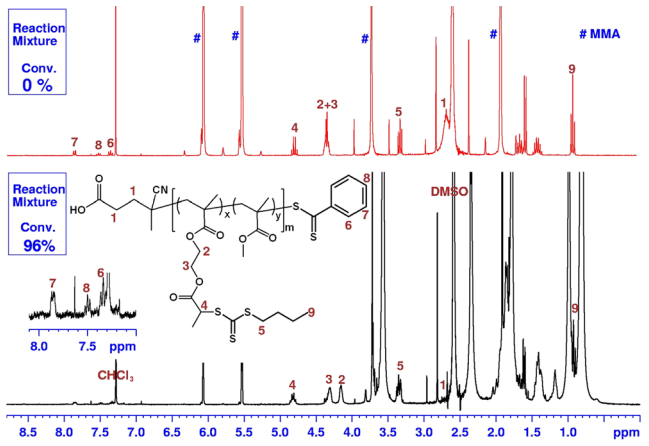

Figure 11. ^{1}H NMR spectra (300 MHz, $CDCl_3$) of the PET-RAFT reaction mixture at different monomer conversions: 0% (red curve, top) and 96% (black curve, bottom). Reaction conditions: light source: 690 nm red LED light (2 mW/cm^2); [MMA]/[BTPEMA]/[CPADB]/[PheoA]/[ZnTPP] = 200:5:1:0.0004:0.02 (2 ppm PheoA and 100 ppm ZnTPP relative to monomer concentration); [MMA]$_0$ = 4.7 mol/L; conversion = 96%; $M_{n,GPC}$ = 23 020 g/mol; M_w/M_n = 1.18.

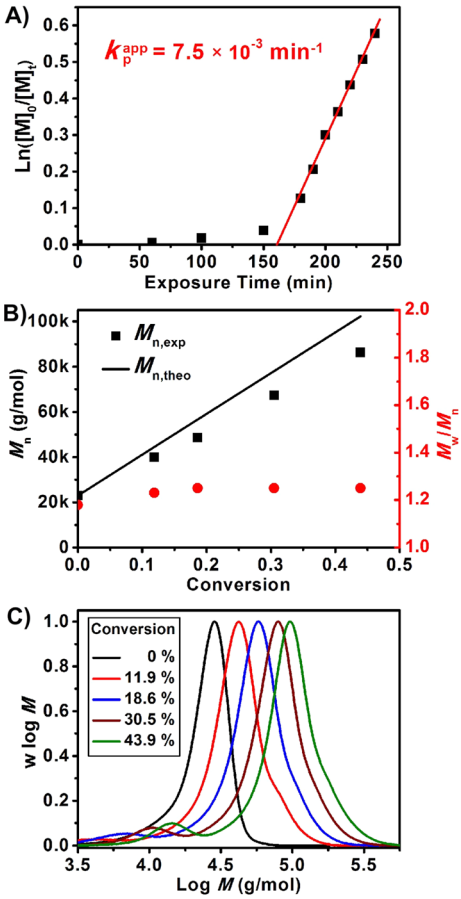

Figure 12. Kinetic study of the grafting photopolymerization of MA using P(MMA-*r*-BTPEMA) as the macroinitiator in the presence of ZnTPP and PheoA under green light (λ_{max} = 530 nm, 0.6 mW/cm^2): (A) ln([M]$_0$/[M]$_t$) vs time of exposure; (B) $M_{n,exp}$ (■), $M_{n,th}$ based on trithiocarbonate only (solid line), and M_w/M_n (●) vs conversion; (C) molecular weight distributions at different monomer conversions. Reaction conditions: [MA]/[P(MMA-*r*-BTPEMA)]/[PheoA]/[ZnTPP] = 2100:1:0.0004:0.02 (10 ppm ZnTPP relative to monomer concentration); molecular weight of P(MMA-*r*-BTPEMA): $M_{n,GPC}$ = 23 020 g/mol; M_w/M_n = 1.18; [MA]$_0$ = 1.2 mol/L; polystyrene standard for molecular weight calibration; low molecular weight (<15 000 g/mol) peak was excluded in determining M_w/M_n.

to build complex macromolecules through a one-pot, two-step process without intermittent postmodification or purification and only a simple flick of the light switch, as shown in Scheme 3. First, the methacrylate, 2-(2-(*n*-butyltrithiocarbonate)-propionate)ethyl methacrylate (BTPEMA; Scheme S2; ^{1}H and ^{13}C NMR are shown in Figures S26 and S27), containing a trithiocarbonate functional group was synthesized. This monomer was co-polymerized with MMA in the presence of CPADB, PheoA, and ZnTPP under 690 nm red light irradiation (2 mW/cm^2) using [MMA]/[BTPEMA]/[CPADB]/[PheoA]/[ZnTPP] = 200:5:1:0.0004:0.02 (2 ppm PheoA and 100 ppm ZnTPP relative to monomer concentration). With light irradiation, the polymerization proceeded smoothly and reached 96% conversion after 30 h. The purified product appeared brown and exhibited UV−vis absorption characteristics of both dithiobenzoate and trithiocarbonate (Figure 2). In the kinetic study, the linear plot of ln([M]$_0$/[M]$_t$) against exposure time suggested a constant radical concentration and robust catalyst activity (Figure 10A). After 30 h of red light exposure, the living features of the polymerization were

DOI: 10.1021/jacs.5b12408
J. Am. Chem. Soc. 2016, 138, 3094−3106

evidenced by the good agreement between the experimental and theoretical values, with low polydispersities (<1.2) (Figure 10B) and with CPADB as the only reacted RAFT agent. The GPC curves (Figure 10C) showed a clear shift to high molecular weights with increasing conversion of monomer, although low molecular weight tailing became observable at high monomer conversion (96%). In addition, the ^{1}H NMR spectrum (Figure 11) of the reaction mixture at 96% monomer conversion revealed the presence of dithiobenzoate (δ 7.2−8.0 ppm). The presence of a proton signal at δ 4.8 ppm assigned to the trithiocarbonate moiety also suggested that trithiocarbonate was not involved in the polymerization of MMA.

Following the successful formation of the methacrylate backbone, the second monomer, MA, was added into the reaction mixture along with DMSO for dilution, and the mixture was placed under green light irradiation. The polymerization kinetics were investigated by online FTNIR spectroscopy. The kinetics demonstrated temporal control (Figure S28) and molecular weight control with low polydispersity (<1.25 up to 43.9% monomer conversion) (Figure 12B), which verified the successful preparation of graft co-polymers. The low molecular weight peak (M_n < 15 000 g/mol) in GPC curves for the graft co-polymer in Figure 12C, which increased during the polymerization, is attributed to a small amount of intrapolymer coupling byproduct or low molecular weight dead PMMA chain with one or two trithiocarbonate side groups. The end group fidelity studied with high-resolution 600 MHz ^{1}H NMR (Figure 13) for the purified final graft co-polymer clearly showed dithiobenzoate and trithiocarbonate end groups.

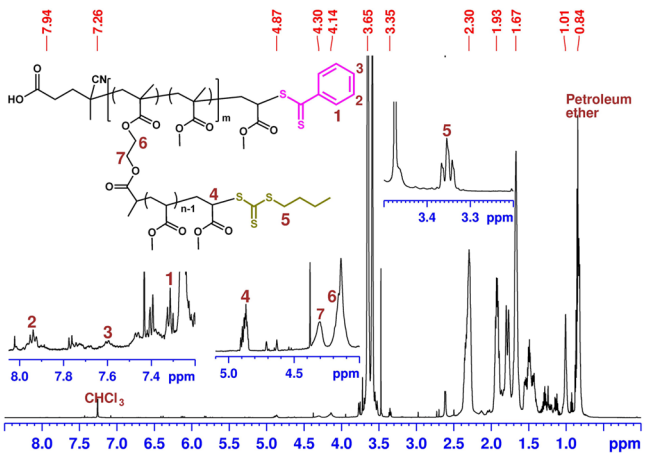

Figure 13. High-resolution ^{1}H NMR spectrum (600 MHz, $CDCl_3$) of purified graft polymer P(MMA-*r*-BTPEMA)-*g*-PMA prepared by PET-RAFT polymerization of MA in the presence of P(MMA-*r*-BTPEMA) ($M_{n,GPC}$ = 23 020 g/mol; M_w/M_n = 1.18) as the macroinitiator. [MA]/[P(MMA-*r*-BTPEMA)]/[PheoA]/[ZnTPP] = 2100:1:0.0004:0.02 (10 ppm ZnTPP relative to monomer concentration); $[MA]_0$ = 1.2 mol/L; conversion = 43.9%; $M_{n,GPC}$ = 86 260 g/mol; M_w/M_n = 1.25.

CONCLUSIONS

In summary, visible-light-mediated selective photoactivation of RAFT agents provides a general strategy for the construction of precise (macro)molecular architectures. The selectivity and efficiency of PheoA to mediate a PET process were illustrated by a simple organic transformation (single unit monomer insertion) and for the synthesis of complex macromolecular structures (graft co-polymers). Single unit monomer insertion into dithiobenzoate was successfully performed using PheoA with a high yield and in the absence of side reactions and byproducts for three monomer families. A novel route to polymer architectures (graft co-polymers) through selective photoactivation was developed based on the highly orthogonal selectivity of two photoredox catalysts, PheoA and ZnTPP, and their specific activation wavelength. PheoA displayed specificity toward the activation of CPADB for the polymerization of methacrylates under red light, and ZnTPP was utilized for the selective activation of trithiocarbonate for the polymerization of acrylate side chains under green light. Thereby, a graft co-polymer comprising a polymethacrylate backbone and polyacrylate graft chains was successfully prepared in one pot by switching the wavelength of the light (red to green). This approach provides new avenues for the development of advanced architectures[102,107−109] requiring higher degrees of control.

ASSOCIATED CONTENT

Supporting Information

The Supporting Information is available free of charge on the ACS Publications website at DOI: 10.1021/jacs.5b12408.

Experimental details, UV−vis spectra, GPC curves, and NMR spectra (PDF)

AUTHOR INFORMATION

Corresponding Authors

*j.xu@unsw.edu.au (J.X.)
*cboyer@unsw.edu.au (C.B.)

Notes

The authors declare no competing financial interest.

ACKNOWLEDGMENTS

The authors thank UNSW for funding. C.B. acknowledges Australian Research Council (ARC) for his Future Fellowship (F12010096).

REFERENCES

(1) Ciamician, G. *Science* **1912**, *36*, 385.
(2) Brown, D. R.; La Marche, J. L.; Spanner, G. E. *J. Sol. Energy Eng.* **1992**, *114*, 212.
(3) Schultz, D. M.; Yoon, T. P. *Science* **2014**, *343*, 1239176.
(4) Hoffmann, N. *Chem. Rev.* **2008**, *108*, 1052.
(5) Nicewicz, D. A.; MacMillan, D. W. C. *Science* **2008**, *322*, 77.
(6) Pirnot, M. T.; Rankic, D. A.; Martin, D. B. C.; MacMillan, D. W. C. *Science* **2013**, *339*, 1593.
(7) Terrett, J. A.; Clift, M. D.; MacMillan, D. W. C. *J. Am. Chem. Soc.* **2014**, *136*, 6858.
(8) Wallentin, C. J.; Nguyen, J. D.; Finkbeiner, P.; Stephenson, C. R. J. *J. Am. Chem. Soc.* **2012**, *134*, 8875.
(9) Dai, C.; Narayanam, J. M. R.; Stephenson, C. R. J. *Nat. Chem.* **2011**, *3*, 140.
(10) Du, J.; Skubi, K. L.; Schultz, D. M.; Yoon, T. P. *Science* **2014**, *344*, 392.
(11) Blum, T. R.; Zhu, Y.; Nordeen, S. A.; Yoon, T. P. *Angew. Chem., Int. Ed.* **2014**, *53*, 11056.
(12) Ghosh, I.; Ghosh, T.; Bardagi, J. I.; König, B. *Science* **2014**, *346*, 725.
(13) Prasad Hari, D.; Hering, T.; König, B. *Angew. Chem., Int. Ed.* **2014**, *53*, 725.
(14) Narayanam, J. M. R.; Stephenson, C. R. J. *Chem. Soc. Rev.* **2011**, *40*, 102.

DOI: 10.1021/jacs.5b12408
J. Am. Chem. Soc. 2016, 138, 3094−3106

(15) Prier, C. K.; Rankic, D. A.; MacMillan, D. W. C. *Chem. Rev.* **2013**, *113*, 5322.
(16) Jeffrey, J. L.; Petronijević, F. R.; MacMillan, D. W. C. *J. Am. Chem. Soc.* **2015**, *137*, 8404.
(17) Devery, J. J.; Stephenson, C. R. J. *Nature* **2015**, *519*, 42.
(18) Zuo, Z.; Ahneman, D. T.; Chu, L.; Terrett, J. A.; Doyle, A. G.; MacMillan, D. W. C. *Science* **2014**, *345*, 437.
(19) Romero, N. A.; Margrey, K. A.; Tay, N. E.; Nicewicz, D. A. *Science* **2015**, *349*, 1326.
(20) Esser, P.; Pohlmann, B.; Scharf, H.-D. *Angew. Chem., Int. Ed. Engl.* **1994**, *33*, 2009.
(21) Xiao, P.; Zhang, J.; Dumur, F.; Tehfe, M. A.; Morlet-Savary, F.; Graff, B.; Gigmes, D.; Fouassier, J. P.; Lalevée, J. *Prog. Polym. Sci.* **2015**, *41*, 32.
(22) Yagci, Y.; Jockusch, S.; Turro, N. J. *Macromolecules* **2010**, *43*, 6245.
(23) Tehfe, M.-A.; Dumur, F.; Graff, B.; Gigmes, D.; Fouassier, J.-P.; Lalevée, J. *Macromolecules* **2013**, *46*, 3332.
(24) Avens, H. J.; Bowman, C. N. *J. Polym. Sci., Part A: Polym. Chem.* **2009**, *47*, 6083.
(25) Bowman, C. N.; Kloxin, C. J. *AIChE J.* **2008**, *54*, 2775.
(26) Ohtsuki, A.; Lei, L.; Tanishima, M.; Goto, A.; Kaji, H. *J. Am. Chem. Soc.* **2015**, *137*, 5610.
(27) Anastasaki, A.; Nikolaou, V.; Zhang, Q.; Burns, J.; Samanta, S. R.; Waldron, C.; Haddleton, A. J.; McHale, R.; Fox, D.; Percec, V.; Wilson, P.; Haddleton, D. M. *J. Am. Chem. Soc.* **2014**, *136*, 1141.
(28) Treat, N. J.; Sprafke, H.; Kramer, J. W.; Clark, P. G.; Barton, B. E.; Read de Alaniz, J.; Fors, B. P.; Hawker, C. J. *J. Am. Chem. Soc.* **2014**, *136*, 16096.
(29) Xu, J. T.; Jung, K.; Atme, A.; Shanmugam, S.; Boyer, C. *J. Am. Chem. Soc.* **2014**, *136*, 5508.
(30) Fors, B. P.; Hawker, C. J. *Angew. Chem., Int. Ed.* **2012**, *51*, 8850.
(31) Yang, Q.; Dumur, F.; Morlet-Savary, F.; Poly, J.; Lalevée, J. *Macromolecules* **2015**, *48*, 1972.
(32) Pan, X.; Lamson, M.; Yan, J.; Matyjaszewski, K. *ACS Macro Lett.* **2015**, *4*, 192.
(33) Frick, E.; Anastasaki, A.; Haddleton, D. M.; Barner-Kowollik, C. *J. Am. Chem. Soc.* **2015**, *137*, 6889.
(34) Chen, M.; MacLeod, M. J.; Johnson, J. A. *ACS Macro Lett.* **2015**, *4*, 566.
(35) Anastasaki, A.; Nikolaou, V.; Simula, A.; Godfrey, J.; Li, M.; Nurumbetov, G.; Wilson, P.; Haddleton, D. M. *Macromolecules* **2014**, *47*, 3852.
(36) Konkolewicz, D.; Schröder, K.; Buback, J.; Bernhard, S.; Matyjaszewski, K. *ACS Macro Lett.* **2012**, *1*, 1219.
(37) Morris, J.; Telitel, S.; Fairfull-Smith, K. E.; Bottle, S. E.; Lalevee, J.; Clement, J.-L.; Guillaneuf, Y.; Gigmes, D. *Polym. Chem.* **2015**, *6*, 754.
(38) Perkowski, A. J.; You, W.; Nicewicz, D. A. *J. Am. Chem. Soc.* **2015**, *137*, 7580.
(39) Lalevée, J.; Tehfe, M.-A.; Zein-Fakih, A.; Ball, B.; Telitel, S.; Morlet-Savary, F.; Graff, B.; Fouassier, J. P. *ACS Macro Lett.* **2012**, *1*, 802.
(40) Dadashi-Silab, S.; Aydogan, C.; Yagci, Y. *Polym. Chem.* **2015**, *6*, 6595.
(41) Telitel, S.; Dumur, F.; Telitel, S.; Soppera, O.; Lepeltier, M.; Guillaneuf, Y.; Poly, J.; Morlet-Savary, F.; Fioux, P.; Fouassier, J.-P.; Gigmes, D.; Lalevee, J. *Polym. Chem.* **2015**, *6*, 613.
(42) Xiao, P.; Dumur, F.; Graff, B.; Gigmes, D.; Fouassier, J. P.; Lalevée, J. *Macromol. Rapid Commun.* **2013**, *34*, 1452.
(43) Ogawa, K. A.; Goetz, A. E.; Boydston, A. J. *J. Am. Chem. Soc.* **2015**, *137*, 1400.
(44) Goetz, A. E.; Boydston, A. J. *J. Am. Chem. Soc.* **2015**, *137*, 7572.
(45) Fors, B. P.; Poelma, J. E.; Menyo, M. S.; Robb, M. J.; Spokoyny, D. M.; Kramer, J. W.; Waite, J. H.; Hawker, C. J. *J. Am. Chem. Soc.* **2013**, *135*, 14106.
(46) Xu, J. T.; Jung, K.; Corrigan, N. A.; Boyer, C. *Chem. Sci.* **2014**, *5*, 3568.
(47) Xu, J.; Shanmugam, S.; Duong, H. T.; Boyer, C. *Polym. Chem.* **2015**, *6*, 5615.
(48) Shanmugam, S.; Xu, J. T.; Boyer, C. *Chem. Sci.* **2015**, *6*, 1341.
(49) Shanmugam, S.; Xu, J.; Boyer, C. *J. Am. Chem. Soc.* **2015**, *137*, 9174.
(50) Leibfarth, F. A.; Mattson, K. M.; Fors, B. P.; Collins, H. A.; Hawker, C. J. *Angew. Chem., Int. Ed.* **2013**, *52*, 199.
(51) Zhao, Y.; Zhang, S.; Wu, Z.; Liu, X.; Zhao, X.; Peng, C.-H.; Fu, X. *Macromolecules* **2015**, *48*, 5132.
(52) Zhang, H.; Deng, J.; Lu, L.; Cai, Y. *Macromolecules* **2007**, *40*, 9252.
(53) Miyake, G. M.; Theriot, J. C. *Macromolecules* **2014**, *47*, 8255.
(54) Sheng, W.; Li, B.; Wang, X.; Dai, B.; Yu, B.; Jia, X.; Zhou, F. *Chem. Sci.* **2015**, *6*, 2068.
(55) Liu, G.; Shi, H.; Cui, Y.; Tong, J.; Zhao, Y.; Wang, D.; Cai, Y. *Polym. Chem.* **2013**, *4*, 1176.
(56) Shi, Y.; Gao, H.; Lu, L.; Cai, Y. *Chem. Commun.* **2009**, 1368.
(57) Shi, Y.; Liu, G.; Gao, H.; Lu, L.; Cai, Y. *Macromolecules* **2009**, *42*, 3917.
(58) Ciftci, M.; Tasdelen, M. A.; Li, W.; Matyjaszewski, K.; Yagci, Y. *Macromolecules* **2013**, *46*, 9537.
(59) Chen, M.; Johnson, J. A. *Chem. Commun.* **2015**, *51*, 6742.
(60) Teator, A. J.; Lastovickova, D. N.; Bielawski, C. W. *Chem. Rev.* **2015**, DOI: 10.1021/acs.chemrev.5b00426.
(61) Hirschbiel, A. F.; Konrad, W.; Schulze-Sünninghausen, D.; Wiedmann, S.; Luy, B.; Schmidt, B. V. K. J.; Barner-Kowollik, C. *ACS Macro Lett.* **2015**, *4*, 1062.
(62) Tan, J.; Sun, H.; Yu, M.; Sumerlin, B. S.; Zhang, L. *ACS Macro Lett.* **2015**, *4*, 1249.
(63) Oehlenschlaeger, K. K.; Mueller, J. O.; Heine, N. B.; Glassner, M.; Guimard, N. K.; Delaittre, G.; Schmidt, F. G.; Barner-Kowollik, C. *Angew. Chem., Int. Ed.* **2013**, *52*, 762.
(64) Kaupp, M.; Tischer, T.; Hirschbiel, A. F.; Vogt, A. P.; Geckle, U.; Trouillet, V.; Hofe, T.; Stenzel, M. H.; Barner-Kowollik, C. *Macromolecules* **2013**, *46*, 6858.
(65) Tasdelen, M. A.; Yagci, Y. *Angew. Chem., Int. Ed.* **2013**, *52*, 5930.
(66) Treat, N. J.; Fors, B. P.; Kramer, J. W.; Christianson, M.; Chiu, C.-Y.; Alaniz, J. R. d.; Hawker, C. J. *ACS Macro Lett.* **2014**, *3*, 580.
(67) Xu, J.; Jung, K.; Boyer, C. *Macromolecules* **2014**, *47*, 4217.
(68) Yeow, J.; Xu, J.; Boyer, C. *ACS Macro Lett.* **2015**, *4*, 984.
(69) Jung, K.; Xu, J.; Zetterlund, P. B.; Boyer, C. *ACS Macro Lett.* **2015**, *4*, 1139.
(70) Shanmugam, S.; Boyer, C. *J. Am. Chem. Soc.* **2015**, *137*, 9988.
(71) McLeary, J. B.; Calitz, F. M.; McKenzie, J. M.; Tonge, M. P.; Sanderson, R. D.; Klumperman, B. *Macromolecules* **2004**, *37*, 2383.
(72) Zard, S. Z. *Angew. Chem., Int. Ed. Engl.* **1997**, *36*, 672.
(73) Chen, M.; Ghiggino, K. P.; Mau, A. W. H.; Rizzardo, E.; Sasse, W. H. F.; Thang, S. H.; Wilson, G. J. *Macromolecules* **2004**, *37*, 5479.
(74) Chen, M.; Ghiggino, K. P.; Rizzardo, E.; Thang, S. H.; Wilson, G. J. *Chem. Commun.* **2008**, 1112.
(75) Zamfir, M.; Lutz, J.-F. *Nat. Commun.* **2012**, *3*, 1138.
(76) Vandenbergh, J.; Reekmans, G.; Adriaensens, P.; Junkers, T. *Chem. Sci.* **2015**, *6*, 5753.
(77) Vandenbergh, J.; Reekmans, G.; Adriaensens, P.; Junkers, T. *Chem. Commun.* **2013**, *49*, 10358.
(78) Graeme, M.; Carlos, G.-S.; Joris, J. H.; Daniel, J. K.; Almar, P.; Ezio, R.; San, H. T. In *Sequence-Controlled Polymers: Synthesis, Self-Assembly, and Properties*; Lutz, J.-F., Meyer, T. Y., Ouchi, M., Sawamoto, M., Eds.; American Chemical Society: Washington, DC, 2014; Vol. *1170*, p 133.
(79) Haven, J. J.; Vandenbergh, J.; Kurita, R.; Gruber, J.; Junkers, T. *Polym. Chem.* **2015**, *6*, 5752.
(80) Houshyar, S.; Keddie, D. J.; Moad, G.; Mulder, R. J.; Saubern, S.; Tsanaktsidis, J. *Polym. Chem.* **2012**, *3*, 1879.
(81) Moad, G.; Chong, Y. K.; Postma, A.; Rizzardo, E.; Thang, S. H. *Polymer* **2005**, *46*, 8458.
(82) Hill, M. R.; Carmean, R. N.; Sumerlin, B. S. *Macromolecules* **2015**, *48*, 5459.

DOI: 10.1021/jacs.5b12408
J. Am. Chem. Soc. 2016, 138, 3094−3106

(83) Munkholm, C.; Parkinson, D. R.; Walt, D. R. *J. Am. Chem. Soc.* **1990**, *112*, 2608.
(84) Turro, N. J. *Modern Molecular Photochemistry*; Benjamin/Cummings: Menlo Park, CA, 1978.
(85) Stiel, H.; Marlow, I.; Roeder, B. *J. Photochem. Photobiol., B* **1993**, *17*, 181.
(86) Meahcov, L.; Sandu, I. *J. Fluoresc.* **2004**, *14*, 181.
(87) Tucker, J. W.; Stephenson, C. R. J. *J. Org. Chem.* **2012**, *77*, 1617.
(88) Demas, J. N.; Harris, E. W.; McBride, R. P. *J. Am. Chem. Soc.* **1977**, *99*, 3547.
(89) Kovacic, P.; Kiser, P. F.; Smith, K. M.; Feinberg, B. A. *J. Electroanal. Chem. Interfacial Electrochem.* **1991**, *320*, 415.
(90) Kalyanasundaram, K. *Coord. Chem. Rev.* **1982**, *46*, 159.
(91) Kwak, Y.; Nicolaÿ, R.; Matyjaszewski, K. *Aust. J. Chem.* **2009**, *62*, 1384.
(92) Pan, J.; Xu, Y.; Sun, L.; Sundström, V.; Polívka, T. *J. Am. Chem. Soc.* **2004**, *126*, 3066.
(93) Xu, J.; Shanmugam, S.; Boyer, C. *ACS Macro Lett.* **2015**, *4*, 926.
(94) Wasielewski, M. R.; Liddell, P. A.; Barrett, D.; Moore, T. A.; Gust, D. *Nature* **1986**, *322*, 570.
(95) Soejima, T.; Satoh, K.; Kamigaito, M. *ACS Macro Lett.* **2015**, *4*, 745.
(96) Henry, S. M.; Convertine, A. J.; Benoit, D. S. W.; Hoffman, A. S.; Stayton, P. S. *Bioconjugate Chem.* **2009**, *20*, 1122.
(97) van den Dungen, E. T. A.; Matahwa, H.; McLeary, J. B.; Sanderson, R. D.; Klumperman, B. *J. Polym. Sci., Part A: Polym. Chem.* **2008**, *46*, 2500.
(98) Xu, J.; Shanmugam, S.; Corrigan, N. A.; Boyer, C. In *Controlled Radical Polymerization: Mechanisms*; Matyjaszewski, K., Sumerlin, B. S., Tsarevsky, N. V., Chiefari, J., Eds.; American Chemical Society: Washington, DC, 2015; Vol. *1187*, p 247.
(99) McKenzie, T. G.; Fu, Q.; Wong, E. H. H.; Dunstan, D. E.; Qiao, G. G. *Macromolecules* **2015**, *48*, 3864.
(100) Miura, Y.; Satoh, K.; Kamigaito, M.; Okamoto, Y. *Polym. J.* **2006**, *38*, 930.
(101) Matyjaszewski, K.; Tsarevsky, N. V. *J. Am. Chem. Soc.* **2014**, *136*, 6513.
(102) Sheiko, S. S.; Sumerlin, B. S.; Matyjaszewski, K. *Prog. Polym. Sci.* **2008**, *33*, 759.
(103) Kaneyoshi, H.; Inoue, Y.; Matyjaszewski, K. *Macromolecules* **2005**, *38*, 5425.
(104) Coessens, V.; Pintauer, T.; Matyjaszewski, K. *Prog. Polym. Sci.* **2001**, *26*, 337.
(105) Jiang, X.; Li, Y.; Lu, G.; Huang, X. *Polym. Chem.* **2013**, *4*, 1402.
(106) Semsarilar, M.; Perrier, S. *Nat. Chem.* **2010**, *2*, 811.
(107) Li, X.; Qian, Y.; Liu, T.; Hu, X.; Zhang, G.; You, Y.; Liu, S. *Biomaterials* **2011**, *32*, 6595.
(108) Blencowe, A.; Tan, J. F.; Goh, T. K.; Qiao, G. G. *Polymer* **2009**, *50*, 5.
(109) Li, Y.; Yu, H.; Qian, Y.; Hu, J.; Liu, S. *Adv. Mater.* **2014**, *26*, 6734.

DOI: 10.1021/jacs.5b12408
J. Am. Chem. Soc. 2016, 138, 3094−3106